applied sciences

MDPI

Article

Synergistic Effects of Dielectric Barrier Discharge Plasma Treatment on Hemp Fiber Surface Modification and Mechanical Properties of Hemp-Fiber-Reinforced Epoxy Composites

Choncharoen Sawangrat [1,†], Kittisak Jantanasakulwong [2,3,†], Jonghwan Suhr [4], Kannikar Kaewapai [5], Thidarat Kanthiya [2], Parichat Thipchai [6], Pornchai Rachtanapun [2,3,*] and Pitiwat Wattanachai [7,*]

[1] Department of Industrial Engineering, Faculty of Engineering, Chiang Mai University, Chiang Mai 50200, Thailand; choncharoen@step.cmu.ac.th
[2] Division of Packaging Technology, School of Agro-Industry, Faculty of Agro-Industry, Chiang Mai University, Mae-Hea, Mueang, Chiang Mai 50100, Thailand; kittisak.jan@cmu.ac.th (K.J.); thidarat.kan@cmu.ac.th (T.K.)
[3] Center of Excellence in Agro Bio-Circular-Green Industry (Agro BCG), Chiang Mai University, Chiang Mai 50100, Thailand
[4] School of Mechanical Engineering, Sungkyunkwan University, 2066 Seobu-ro, Jangan-gu, Suwon-si 16419, Gyeonggi-do, Republic of Korea; suhr@skku.edu
[5] Science and Technology Park (STeP), Chiang Mai University, Chiang Mai 50100, Thailand; kannikar@step.cmu.ac.th
[6] Doctor of Philosophy Program in Nanoscience and Nanotechnology (International Program/Interdisciplinary), Faculty of Science, Chiang Mai University, Chiang Mai 50200, Thailand; parichat_thi@cmu.ac.th
[7] Department of Civil Engineering, Faculty of Engineering, Chiang Mai University, Chiang Mai 50200, Thailand
* Correspondence: pornchai.r@cmu.ac.th (P.R.); pitiwat@step.cmu.ac.th (P.W.); Tel.: +66-63-549-2556 (P.R.); +66-818824228 (P.W.)
† These authors contributed equally to this work.

check for updates

Academic Editors: Lubos Kascak and Emil Spišák

Received: 25 December 2024
Revised: 1 March 2025
Accepted: 3 March 2025
Published: 5 March 2025

Citation: Sawangrat, C.; Jantanasakulwong, K.; Suhr, J.; Kaewapai, K.; Kanthiya, T.; Thipchai, P.; Rachtanapun, P.; Wattanachai, P. Synergistic Effects of Dielectric Barrier Discharge Plasma Treatment on Hemp Fiber Surface Modification and Mechanical Properties of Hemp-Fiber-Reinforced Epoxy Composites. *Appl. Sci.* **2025**, *15*, 2818. https://doi.org/10.3390/app15052818

Abstract: This study focused on improving the mechanical properties of hemp-fiber-reinforced epoxy (HFRE) composites by modifying the surface of hemp fibers (HFs) using dielectric barrier discharge (DBD) plasma treatment. By exposing the fibers to different gas mixtures Ar, Ar+N_2, and Ar+O_2, the surface of the fibers was altered, adding functional groups, increasing surface roughness, and improving crystallinity. The researchers created HFRE composites using both untreated and plasma-treated HF, and then tested their mechanical properties. The results revealed that Ar+O_2 plasma treatment boosted both the tensile strength (by 15.2%) and energy absorption of the composites. To fine-tune the process, the response surface methodology (RSM) was used to determine the most important factors for optimizing the treatment: input power and treatment time. The ideal conditions were found to be 162.63 W of power and 10 min of treatment. These findings highlight the potential of DBD plasma as a reliable method for modifying the surface of hemp fibers, even with changes in the setup or reactor design. Overall, this approach shows great promise for industrial applications, providing an effective way to improve the strength and durability of HFRE composites for a variety of uses.

Keywords: hemp fiber; plasma treatment; dielectric barrier discharge; composite materials; epoxy; mechanical properties

1. Introduction

The exceptional properties in natural-fiber-reinforced composites include the high strength-to-weight ratio, improved durability, and design flexibility [1]. This has resulted in the increasing interest in natural-fiber-reinforced composites due to the increase in demand

for sustainable and eco-friendly materials [2,3]. Hemp fiber (HF) has emerged as one of the potential reinforcing fibers for polymer composites among various natural fibers based on its properties and ecology [3]. Hemp fiber has a greater cellulose content (70–90%) than that of other natural fibers such as sisal, jute, and flax [4,5]. It has a high cellulose content and, therefore, a high modulus and tensile strength of the fiber in mechanical performance [6]. Moreover, HF exhibits a low density (1.48 g/cm^3), which renders HF appropriate for lightweight composite applications [3]. The high strength and low density are suitable for gaining a better specific strength than other conventional reinforcements like glass fiber [7]. Although HF has favorable features for use, its hydrophilic property makes it difficult to serve as reinforcement in hydrophobic polymer matrices [5]. This disparity in surface energy between the fiber and matrix results in weak interfacial bonding which may also restrict the ability of stress transmission and composite mechanical performance [8]. In response to this problem, numerous surface modification strategies have been developed to improve the compatibility and interfacial bonding of HF with polymer matrices. Of these surface modification methods, plasma treatment has received considerable interest owing to its eco-friendliness, efficiency, and versatility [9]. Instead of chemical methods, plasma treatment has advantages such as the fact that it consumes less time than chemical methods, is low-energy, and causes less environmental impact [10]. Dielectric barrier discharge (DBD) plasma, a type of atmospheric plasma, is an especially attractive plasma technology for the continuous processing of fibers and for scalability towards industrial usage [11].

Plasma technology can produce a series of cleaning, etching, polymerization, and crosslinking effects, as well as other complex physical and chemical effects [12]. Plasma treatment leads to diverse changes in the surface of fibers like adding groups and enhancing roughness for better wettability [13,14]. These alterations occur due to the interactions between reactive plasma species and the fiber surface in a manner with factors, like the power level and treatment duration affecting the type and degree of modification. Introducing groups like carbonyls, carboxyl, and hydroxyls onto the surface of fibers through plasma treatment boosts the compatibility and reactivity with the polymer matrix [14]. These functional groups are able to engage in chemical bonding with the matrix which enhances adhesion [15]. Additionally, the increase in surface roughness caused by plasma etching results in a surface area for interlocking between the fiber and matrix [13]. Prior research has shown that using plasma treatment can enhance the strength of composites made from fibers [13,16]. However, there is a need for an investigation into how to best optimize DBD plasma parameters for surface modification in HF applications specifically. The interplay between plasma treatment effects on HF surfaces and how this impacts the properties of HF-reinforced composites is essential for creating eco-friendly composite materials, with high performance capabilities.

However, the utilization of plasma to process hemp fibers is relatively unstudied, especially considering how plasma affects various constituents like hemicelluloses and lignin. Ramie fibers are the subject of the most research on lignocellulosic fibers and the potential for plasma treatment of these fibers.

Biljana et al. [6] employed the dielectric barrier discharge (DBD) for studying the effects of plasma treatment on the morphology and sorption properties of hemp fibers under different conditions (40 W and 80 W powers at constant treatment time of 120 s). The wettability test of the plasma-treated samples showed a considerable increase compared to untreated fibers, which correlates with the chemical composition change of the processed hemp fiber surface, as demonstrated by the ATR FTIR results, and to the rise in fiber surface roughness owing to the intensive etching visible in the SEM images. Plasma treatment was proven to positively affect the water sorption properties of raw hemp fibers and could replace the use of chemicals for many fiber applications.

Sameer et al. [17] studied the effect of the plasma treatment on the nanoscale surface structure of ramie fibers and their influence on fiber–polymer adhesion. They found filament-like nanostructures on the surface of the ramie fibers within 1 min of plasma treatment. These structures dominate the mechanical properties of the fibers. The consequent nanoscale surface roughness due to the microfibrillation of cellulose increased the surface area, which, in turn, improved the amount of water contained in it as well as the interactions between the fiber and polymer. Thus, using plasma surface modification for fiber–polymer composites can be advantageous for attaining a better interface integrity.

The objective of this research study is to fill the aforementioned knowledge gap by examining the effects of various DBD plasma treatment parameters (treatment time, discharge power, and gas composition) on the surface properties and mechanical characteristics of HF and HF-loaded epoxy composites. Optimizing these parameters through response surface methodology (RSM) can give a significant information to customize the properties of HF composites for particular applications. These results enhance the development of HF-plasma-treated sustainable composite materials. The enhanced interfacial adhesion and mechanical properties obtained by plasma treatment could bring further applications for HF composites in the automotive, construction, and packaging sectors. In addition, DBD plasma treatment is environmentally friendly and in line with the increasing acceptance of green and sustainable manufacturing processes in the composites industry.

2. Materials and Methods

2.1. Materials and Preparation

The bark of hemp (*Cannabis sativa* L.) from Fang District, Chiang Mai Province, Thailand was applied in this study. The hemp stems were mechanically peeled to separate the pure bark, which was later ground into a coarse powder using a commercial grinder (Grinder ML-SC5-III, Ming Lee Industrial Ltd., Hong Kong, China). For the extraction of cellulose from hemp bark, the chemicals used for alkaline treatment and bleaching processes such as, sodium hydroxide (NaOH), and sodium chlorite ($NaClO_2$) (Merck & Co., Inc., Darmstadt, Germany) were laboratory-grade. After bleaching process, the cellulose was dried in a hot air oven at 80 $\pm$ 3 °C for 12 h and kept in a desiccator. Subsequently, the hemp powder was sieved through a 180-micron mesh to achieve a consistent particle size fraction.

2.2. Influence of Plasma Parameters

HF were randomly classified into untreated (HF) and plasma-treated (HF_{tr}). The HF were subjected to plasma treatment under atmospheric pressure using a DBD cell (Minismart, PLASMART., Co., Ltd., Daegeon, Republic of Korea). The DBD plasma generator consists of two plane-parallel electrodes, a powered and grounded electrode, and an RF power supply operated at a frequency of 13.56 MHz. Extracted HF were placed on an aluminum tray, positioned above the grounded electrode, which was moved back and forth at a rate of 30 cm s^{-1}. A schematic of the DBD cell operated under atmospheric pressure is shown in Figure 1. The distance between the powered electrode and sample tray was fixed to maintain a consistent discharge gap of 1 mm.

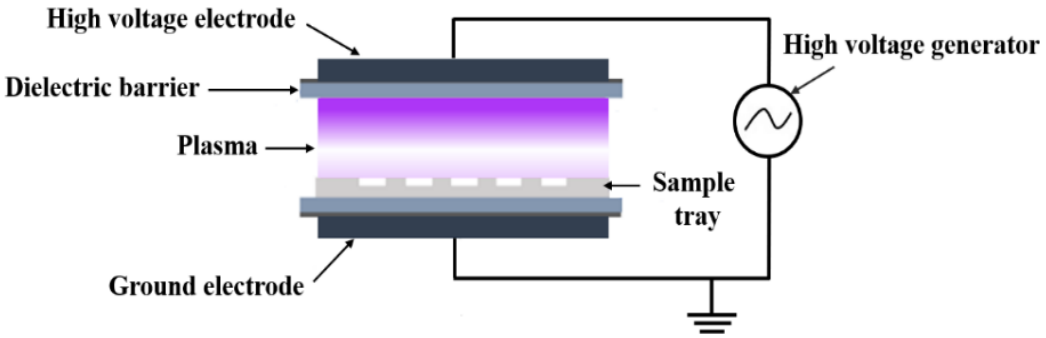

Figure 1. Schematic of the DBD cell operated under atmospheric pressure.

For measuring the effect of the type of plasma gases, the plasma treatment time was 10 min, plasma power 180 W, and the type of gases was argon (Ar), nitrogen (N_2), and oxygen (O_2). The Ar gas was used with flow rates of 8 L min^{-1}, while the O_2 and N_2 gases used were 10 sccm. Samples were treated in triplicate under each condition and stored in foil bags for further analysis. Furthermore, the structural characterization and surface chemical composition of the hemp fibers were thoroughly examined using Fourier-transform infrared (FT-IR) spectroscopy, X-Ray diffraction (XRD) analysis, and scanning electron microscopy (SEM) in conjunction with energy-dispersive X-Ray spectroscopy (EDS).

2.3. Fourier-Transform Infrared Spectroscopy (FT-IR)

FT-IR spectroscopy (FT/IR-4700, JASCO International Co., Ltd., Pfungstadt, Germany) was adopted to analyze surface functionalities of the HF samples, both untreated and plasma-treated. The samples were mixed with KBr and pressed into sheets in a sample holder. The FT-IR spectra were recorded in the range of 500–4000 cm^{-1}.

2.4. X-Ray Diffraction Spectroscopy (XRD)

The crystallinity of the HF and HF_{tr} samples was analyzed using XRD (SmartLab X-ray diffractometer, Rigaku, Ltd., Tokyo, Japan) with the scattering angle (2θ) in the range 10–60°. The crystallinity index (C.I.) was determined with Equation (1).

$$\% \text{ C.I.} = \frac{(I_{002} - I_{am})}{I_{002}} \times 100 \quad (1)$$

where I_{002} is the maximum intensity of the peak corresponding to the 002 plane, and I_{am} is the minimum intensity between the peaks corresponding to the 012 and 002 planes [18].

2.5. Scanning Electron Microscopy (SEM)

The microstructures of the plasma-treated hemp fiber samples were examined using SEM (JSM-IT300, JEOL Ltd., Tokyo, Japan), which was conducted to investigate the surface morphology of the HF and HF_{tr} samples at the micro–nanoscale. Microscale observations were captured at high magnification at an acceleration voltage of 10 kV.

2.6. Preparation of Composite and Mechanical Properties

HF-reinforced epoxy (HFRE) composites and HF_{tr}-reinforced epoxy (HF_{tr}RE) composites samples were prepared by a casting process for tensile testing. The HF and HF_{tr} were incorporated into the epoxy matrix with 5 wt% of the sample mass. The composite fluid was then cast onto a silicone mold using a vacuum technique. The bone-shaped dimensions were measured following the JIS K 6251-7 standard [19] (Figure 2). Tensile properties were evaluated according to the stand for Japanese industrial standards (JIS) by a universal testing machine (MCT-1150, Hounfield Test Equipment, Surrey, UK) at a crosshead speed

of 10 mm/min. Each composite was tested five times to determine its tensile strength and elongation at break. Energy absorption was determined from the average area of the stress–strain curve.

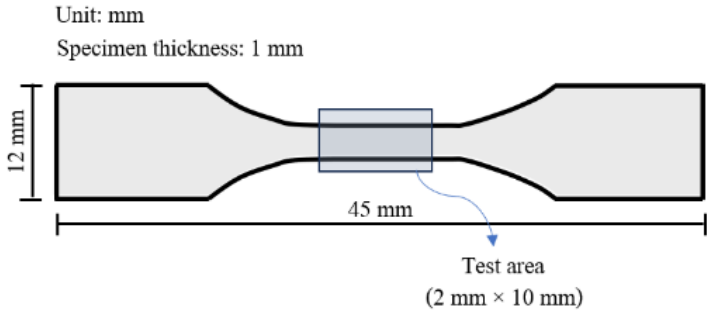

Figure 2. Test specimens for tensile testing according to technical standard.

2.7. Statistical Analysis

All data were analyzed using one-way analysis of variance. Differences were considered significant at the level of $p \leq 0.05$ using the least significant difference (LSD) test. All statistical analyses were conducted using IBM SPSS software version 26.

2.8. Experimental Design and Optimization of Plasma Treatment Parameters

In this study, we investigated the effect of two important plasma treatment parameters, namely, treatment time and discharge power, on the mechanical properties of hemp-fiber-reinforced epoxy (HFRE) composites. The above-mentioned parameters were chosen and retained from previous reports as they have significant influence on the surface modification of natural fibers.

The length of the time exposed to the plasma environment directly correlates with the degree of surface modification and is known as treatment time. Increased treatment duration provides more time for interaction between the reactive plasma species and the fiber surface, facilitating deeper changes in the chemistry and morphology of surface. Yet, treatment times higher than optima can lead to fiber degradation and reduction in mechanical properties. Discharge power, in contrast, affects the density and activity of plasma species. Increasing discharge powers create a harsher plasma environment, which enhanced the modification effects on the surface. However, thermal degradation of the fibers can occur at discharge powers that are too high and deteriorate structural integrity.

A design of experiments (DOE) approach was adopted to optimize these parameters and study their interaction effects on the mechanical properties of HFRE composites using Minitab 21 software. By choosing a full factorial design with factors treatment time and discharge power each at 3 levels, it resulted in an overall of 22 experimental runs listed in Table 1. The levels for treatment time were 10, 30, and 50 min, while the levels for discharge power were 140, 160, and 180 W. The discharge power levels were chosen based on preliminary experiments and literature recommendations within the ranges to achieve adequate surface modification with limited fiber degradation.

Table 1. DBD plasma treatment parameters.

Parameter (unit)	Level of Parameters		
	Low	**Intermediate**	**High**
Discharge Power (W)	140	160	180
Treatment Time (min)	10	30	50

The response variable, tensile strength of the HFRE composites, was measured for each experimental run to evaluate the effects of the plasma treatment parameters. The obtained data were analyzed using analysis of variance (ANOVA) to determine the statistical significance of each parameter and their interactions. The optimization of the plasma treatment parameters was performed using response surface methodology (RSM) to identify the optimal settings for achieving the highest tensile strength.

3. Results

3.1. Analysis of Reactive Species in the DBD Plasma

Figure 3 displays the intensities of the reactive species generated by the DBD plasma. Optical emission spectroscopy (OES) was used for characterization; typical optical emission spectra were obtained in the wavelength range 260–900 nm. The emission spectra confirmed the presence of atomic Ar, –OH radicals, excited N_2, and O radicals in the plasma [20,21]. Atomic O and –OH radicals likely resulted from the fragmentation of H_2O or the dissociation of O_2 in the surrounding air. Additionally, reactive oxygen species (ROS) and reactive nitrogen species (RNS) might have influenced the intracellular surface either by diffusing into the fiber surface or by inducing new reactive species on the cell surface. Atomic O and –OH are highly reactive radicals that play significant roles in the surface modification process [21]

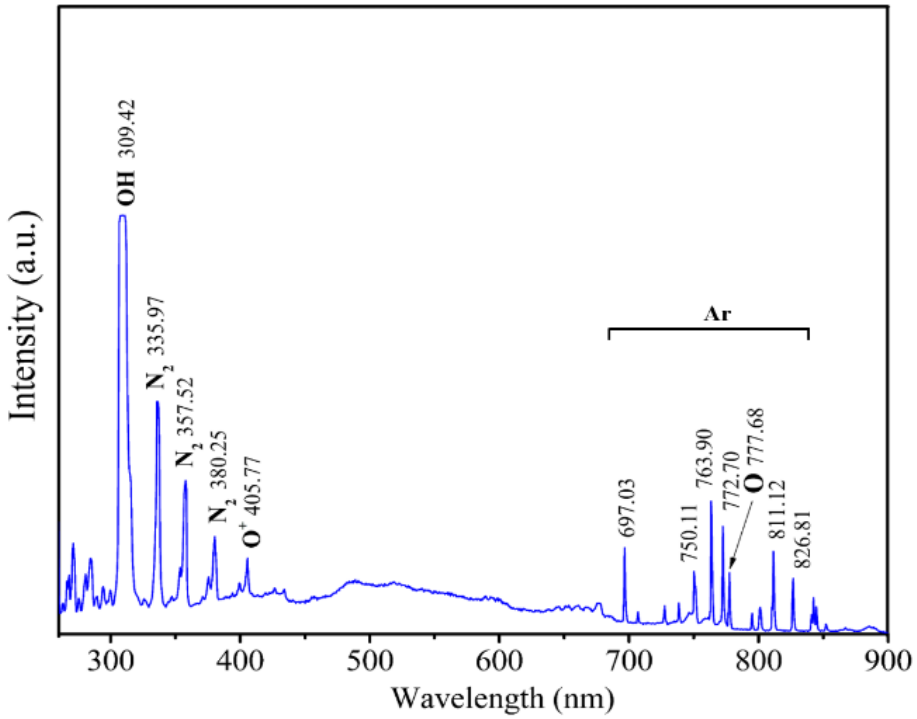

Figure 3. Representative optical emission spectra of the DBD plasma.

3.2. Structural Characterization and Chemical Composition of Hemp Fibers

Crystallographic structure and chemical compositions of untreated hemp fiber (HF) and plasma-treated hemp fibers (HF_{tr}) were studied by X-ray diffraction (XRD) and energy-dispersive X-ray spectroscopy (EDS), respectively. The XRD patterns of HF and HF_{tr} samples (Figure 4) showed characteristic (101) and (002) peaks of cellulose I at 2θ angles of 12.2° and 22.8°, respectively, that are consistent with the literature values [22]. A shoulder at around 20° which corresponds to the (012) plane was also detected, specifying the cellulose II crystalline phase [1,23]. The intensity of the (002) peak, which is the sole crystalline peak for cellulose I, demonstrates considerable amorphous as well as non-crystalline fractions. Table 2 shows the crystallinity index (C.I.) of the plasma-treated HF_{tr}

samples compared to untreated HF samples, showing the highest C.I. values for the N_2 and O_2 plasma-treated HF_{tr} samples. The reason for this higher increase in crystallinity is then attributed to the selective removal of the non-crystalline and amorphous components during the plasma treatment, resulting in a relatively higher amount of crystalline cellulose.

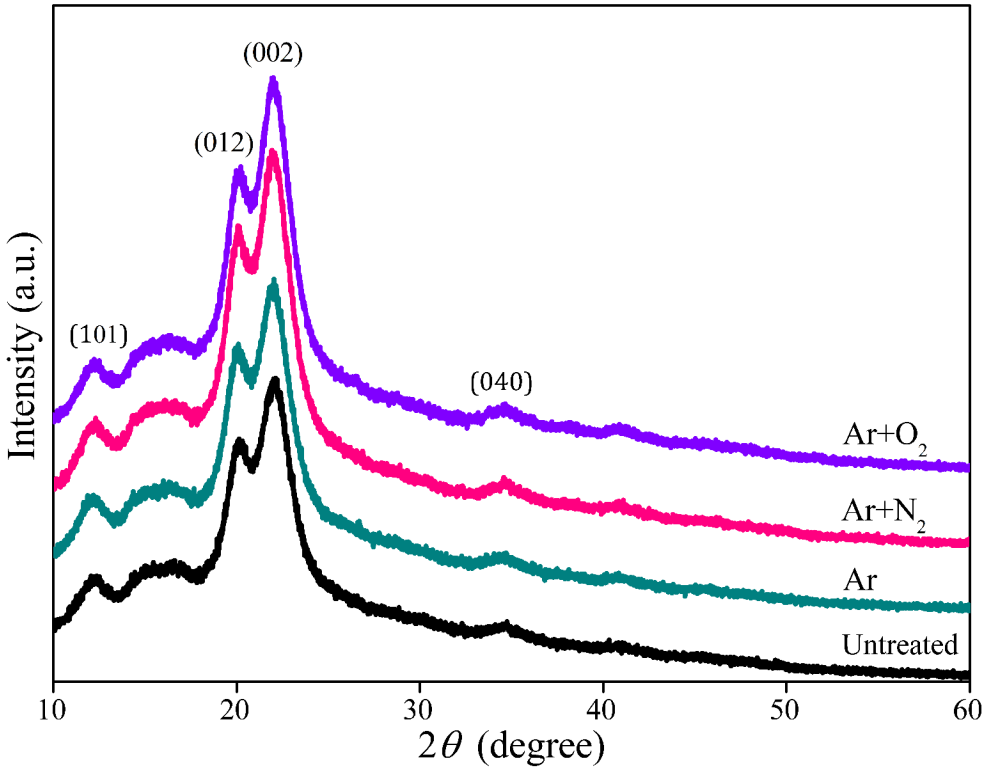

Figure 4. XRD patterns of hemp fiber untreated and treated with Ar, Ar+N_2, and Ar+O_2 plasma.

Table 2. The elemental composition and crystallinity index (C.I.) of the HF and HF_{tr} samples.

Treatments	Compositions (%)		O/C Ratio	C.I. (%)
	C	O		
HF	59.50	40.50	0.68	45.19
HF_{tr} (Ar)	59.03	40.97	0.69	45.20
HF_{tr} (Ar+N_2)	56.17	43.83	0.78	53.86
HF_{tr} (Ar+O_2)	55.96	44.04	0.79	55.63

The results of the EDS analysis (Table 2) also showed that the O/C ratio in the N_2 and O_2 plasma-treated samples was more than the Ar plasma-treated samples. This increase in O/C ratio was attributed to the lowered carbon percent, which probably originated from the etching action involving the non-crystalline cellulose zone with ROS generated in the course of the O_2 plasma treatment.

The FT-IR analysis of the HF and HF_{tr} samples is shown in Figure 5. The stretching vibration band of the hydroxyl group (–OH) which is abundant in cellulose and hemicellulose appeared in the range 3200–3600 cm^{-1}. Finally, the bands at 2900 cm^{-1} were associated with both the CH_2 stretching vibration and the CH group, an indication of the hydrocarbon structure within hemicellulose. The absorption peak at 1640 cm^{-1} demonstrated the adsorbed water molecules in non-crystalline cellulose. The bands at 1430 cm^{-1} and 1369 cm^{-1} were attributed to the C–H deformation of the methoxyl group in lignin and C–H deformation (symmetric), respectively. The band at 1158 and 1060 cm^{-1} show the

C–O stretching of ester groups and the C–OH stretching vibration in cellulose [24]. However, the result showed unique peaks for the main components of hemp fibers like cellulose, hemicellulose, and lignin. No major differences were noted in the spectra of the untreated and treated samples, but the reduction in intensity for the peaks at 3447, 2900, and 1060 cm^{-1} related to the functional structure of hemicellulose, lignin, and amorphous cellulose was found to be more pronounced for N_2 and O_2 plasma-treated samples. This implies that plasma treatment acts selectively; therefore, it can etch and remove these non-cellulosic components at the surface of hemp fibers.

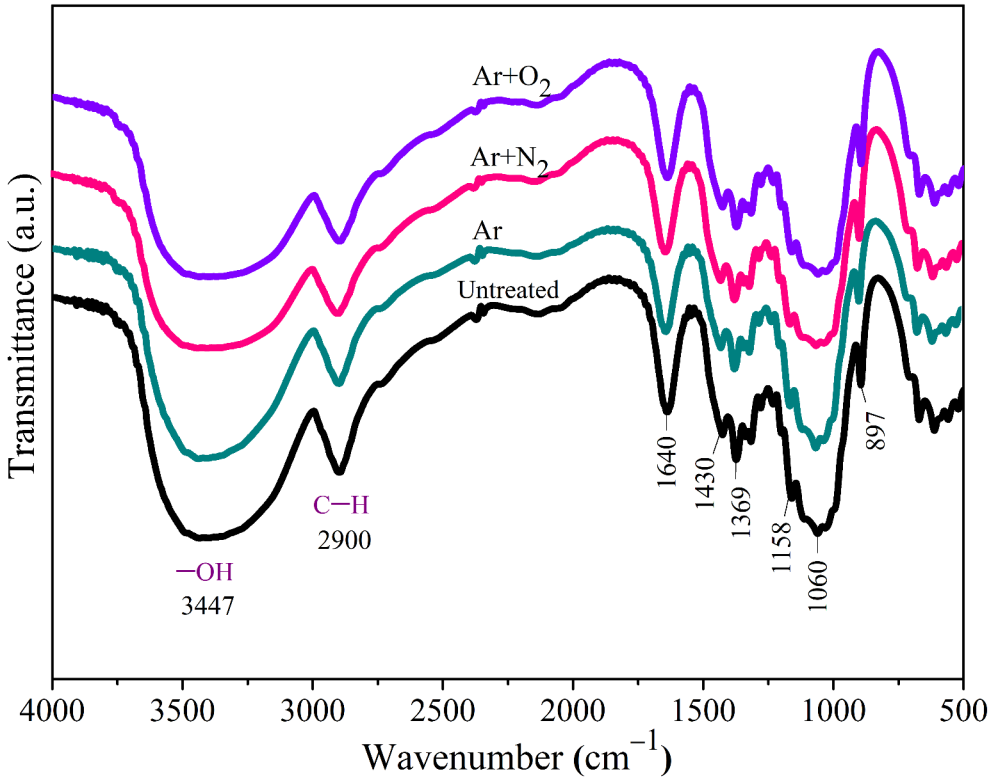

Figure 5. FT-IR spectra of hemp fiber untreated and treated with Ar, Ar+N_2, and Ar+O_2 plasma.

3.3. Surface Morphology and Roughness

Figure 6 shows the surface morphology of untreated HF and HF_{tr} samples scanned by scanning electron microscopy (SEM). The sample with untreated HF showed a microscopically smooth surface with some leftovers or impurities. In contrast, compared to HF_{tr} samples, the samples treated with plasma exhibited significant morphological changes especially for N_2 and O_2 plasma. Due to the presence of an etching effect, the surface roughness increased and microfibrils became exposed as a result of the plasma treatment process; this can be explained by the removal of non-cellulosic components like hemicellulose and lignin from fiber surfaces [25]. The increased surface roughness is critical towards promoting better mechanical interlocking and adhesion between the fibers and matrix [26,27].

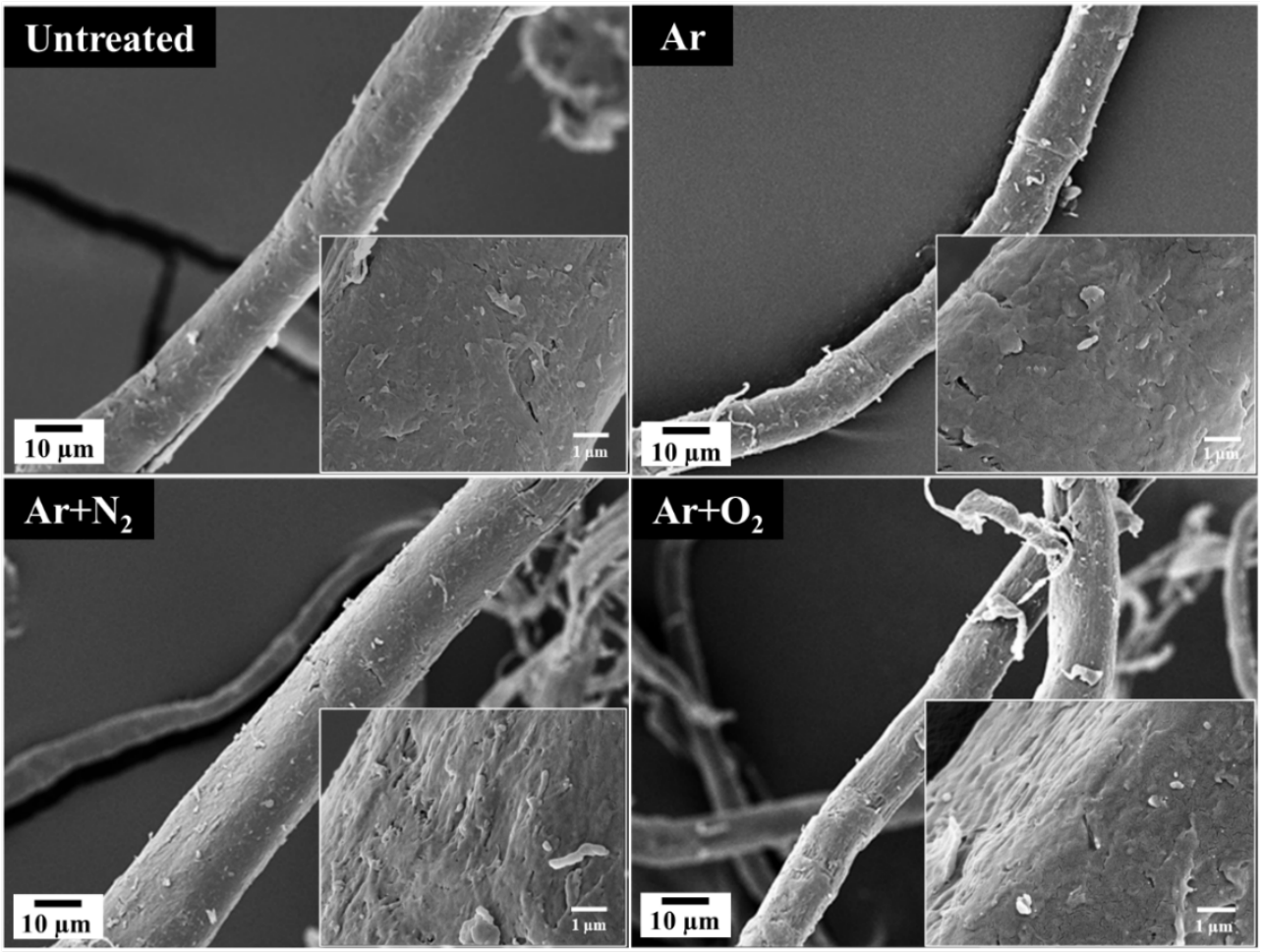

Figure 6. Surface morphology of hemp fiber was untreated and treated with Ar, Ar+N_2, and Ar+O_2 plasma, Note: Main figures before expansion (1000×) and insets show the same images after expansion (15,000×).

The fracture surfaces of the untreated hemp-fiber-reinforced epoxy (HFRE) and plasma-treated hemp-fiber-reinforced epoxy ($HF_{tr}RE$) composites were analyzed using SEM after tensile testing (Figure 7). The untreated HFRE composite exhibited weak interfacial adhesion, as evidenced by the pulling out of fibers from the matrix under external loading, as shown in Figure 7a,d,f.

In contrast, the plasma-treated $HF_{tr}RE$ composites demonstrated enhanced interfacial bonding, as shown in Figure 7b,e,g, which can be attributed to the increased surface roughness of the fibers resulting from the plasma treatment. This improved fiber–matrix interface enables efficient stress transfer and delays failure under external loading conditions.

3.4. Mechanical Properties of Plasma-Treated Hemp Fiber Composites

The tensile properties of the epoxy, HFRE, and $HF_{tr}RE$ composites are shown in Figure 8a and Table 3. The HFRE composite that was used as a reference had a tensile strength of 40.39 ± 0.52 MPa and an elongation at break equal to an average value of 6.27 ± 0.41%.

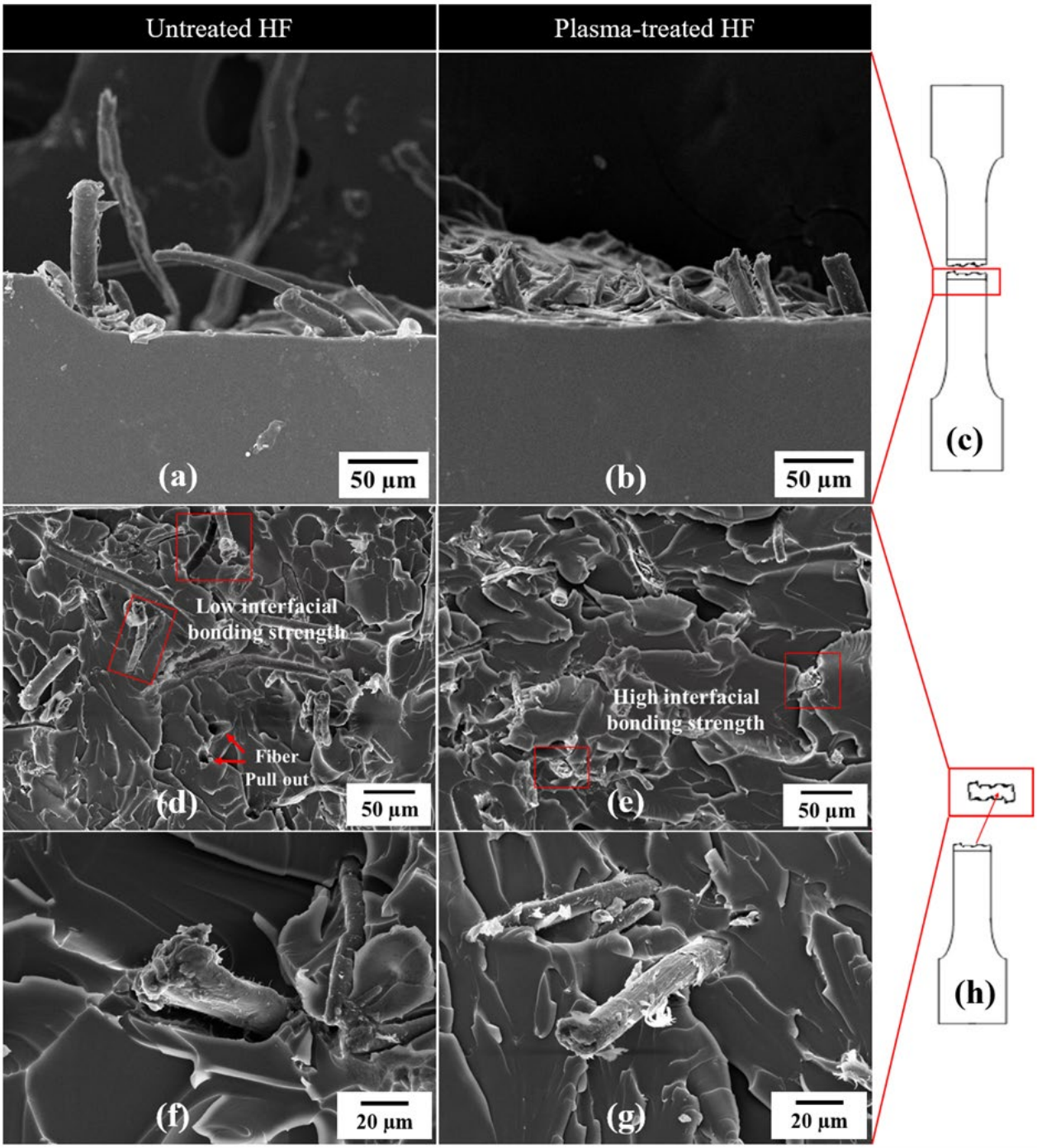

Figure 7. SEM image of (**a**,**b**) cracking patterns of composite samples, (**c**) a model pattern of fracture area observed in side view, (**d**,**e**) a fracture surface overview of composite samples, (**f**,**g**) a fracture surface overview of composite samples after expansion (600×), and (**h**) a model pattern of fracture area observed in top view.

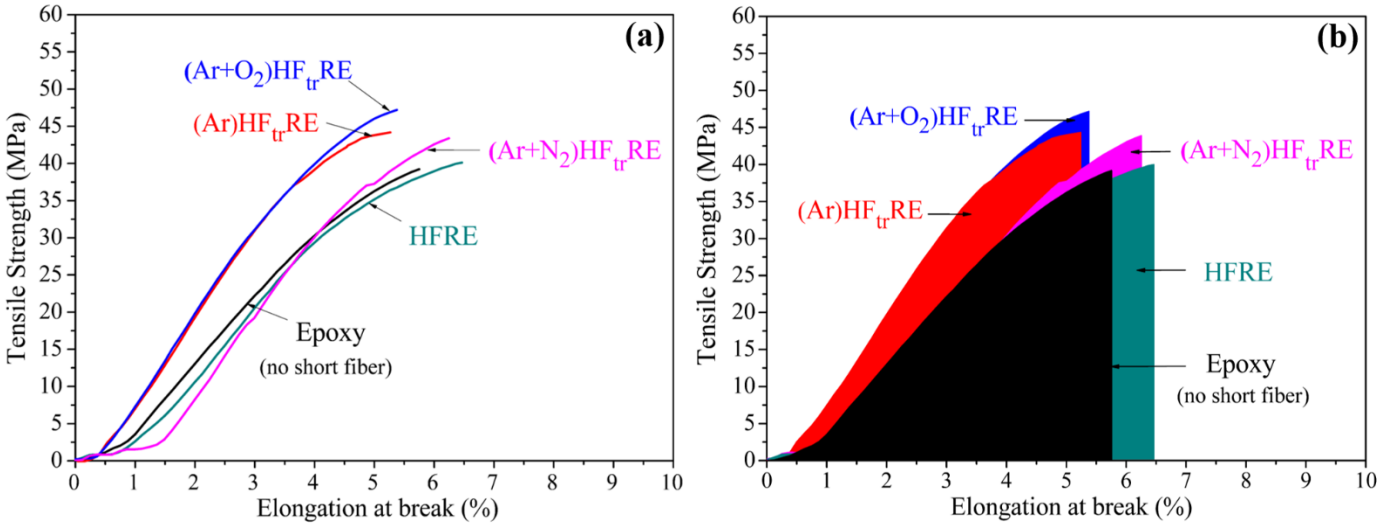

Figure 8. (**a**) Tensile strength and elongation at break and (**b**) calculated energy absorption of the epoxy, the epoxy composite reinforced with untreated HF (HFRE), and the epoxy composite reinforced with plasma-treated HF ($HF_{tr}RE$) in various gasses.

Table 3. Mechanical properties of the HFRE and $HF_{tr}RE$ composite samples.

Sample	Energy Absorption (MPa mm/mm)	Elongation at Break (%)	Tensile Strength (MPa)	Increase Rate of Tensile Value (%)
Epoxy	101.93 ± 6.68^{c}	5.54 ± 0.31^{ab}	39.13 ± 0.29^{e}	-
HFRE	116.01 ± 8.83^{abc}	6.27 ± 0.41^{ab}	40.39 ± 0.52^{d}	-
$(Ar)HF_{tr}RE$	124.01 ± 5.72^{ab}	5.24 ± 0.16^{bc}	44.77 ± 0.35^{b}	10.8
$(Ar+N_2)HF_{tr}RE$	121.32 ± 2.62^{b}	6.09 ± 0.46^{ab}	43.11 ± 0.71^{bc}	6.7
$(Ar+O_2)HF_{tr}RE$	130.64 ± 5.40^{ab}	5.69 ± 0.29^{ab}	46.52 ± 0.54^{a}	15.2

Values in the same column with the same letters are not significantly different at $p \leq 0.05$.

The tensile strength of the $HF_{tr}RE$ composites was also examined, with all plasma-treated samples performing better than control, with the $(Ar+O_2)HF_{tr}RE$ composite having an optimal tensile property for a microscopic increase in the maximum value as 46.52 ± 0.54 MPa, representing a 15.2% increase. The elongation to break values showed no significant difference between the $HF_{tr}RE$ composites and control.

The energy absorption of the composites was calculated by finding areas under stress–strain curves (Figure 8b) as the maximum (130.64 ± 5.40 MPa·mm/mm), which were observed in the case of $(Ar+O_2)HF_{tr}RE$ composites. This significantly improved energy absorption leads to the tensile strength and elongation at break of the composites being increased directly.

These improvements in the mechanical properties can be due to a better interfacial bonding between the plasma-treated hemp fibers and epoxy matrix. This increased surface roughness and exposure of microfibrils on the fiber surface enhances mechanical interlocking and adhesion, leading to efficient stress transfer and delayed failure [28–30].

3.5. Optimization of Plasma Treatment Parameters

A least squares analysis was used to establish a model based on the observation of 22 results from the full factorial experiments. The $HF_{tr}RE$ composite sample's tensile strength, which was impacted by the two factors, was the response variable under investigation. The equation for a second-order polynomial that was produced from the experimental data using quadratic regression models incorporated these factors. The prop-

erties of the epoxy composite reinforced with O_2 plasma-treated HF are comprehensively presented in Table 4, which also highlights the results related to the two variables under investigation and the sample strength.

Table 4. Experimental results based on the DOE method.

Run Order	Center Point	Blocks	Power (W)	Treatment Time (min)	Tensile Strength (MPa)
1	0	1	160	30	41.19
2	1	1	180	10	47.54
3	1	1	140	10	40.26
4	0	1	160	30	44.29
5	0	1	160	30	46.02
6	1	1	140	10	40.24
7	1	1	180	50	44.44
8	0	1	160	30	45.22
9	0	1	160	30	46.54
10	1	1	140	50	23.99
11	1	1	160	30	42.37
12	0	1	160	30	44.35
13	1	1	140	50	42.60
14	0	1	160	30	41.46
15	1	1	140	10	40.24
16	1	1	140	50	36.39
17	0	1	160	30	43.68
18	1	1	180	10	36.88
19	1	1	180	50	41.39
20	0	1	160	30	41.69
21	1	1	180	50	45.54
22	1	1	180	10	41.66

The response surface methodology (RSM) was utilized to optimize the plasma treatment parameters, specifically treatment time and discharge power, with the objective of maximizing the tensile strength of the (Ar+O_2)HF_{tr}RE composites. The analysis of variance (ANOVA) results (Table 5) indicated that the quadratic model was significant ($p < 0.05$), with a coefficient of determination (R-aq) of 44.28%, suggesting a moderate fit between the experimental data and the model.

$$\text{Tensile Strength} = 42.2 - 0.004\ \text{Power} - 0.820\ \text{Treatment time} + 0.00480\ \text{Power*Treatment time} + 3.58\text{CtPt}r \quad (2)$$

Table 5. Analysis of variance of tensile strength of HF_{tr}RE composite sample.

Source	DF	Adj. SS	Adj. Ms	F-Value	*p*-Value
Model	4	222.09	55.52	3.38	0.033
Linear	2	107.77	53.88	3.28	0.063
Power	1	94.81	94.81	5.77	0.028
Treatment time	1	12.96	12.96	0.79	0.387
2-Way Interactions	1	44.28	44.28	2.69	0.119
Power*Treatment time	1	44.28	44.28	2.69	0.119
Curvature	1	70.04	70.04	4.26	0.055
Error	17	279.47	16.44		
Total	21	501.56			
Model Summary					
S	*R*-aq.	*R*-aq. (adj.)	*R*-aq. (pred.)		
4.05455	44.28%	31.17%	0.00%		

The multiple response prediction plot (Figure 9) revealed that the optimal plasma treatment parameters for achieving the maximum tensile strength of 44.77 MPa were a treatment time of 10 min and a discharge power of 162.63 W. These optimized parameters strike a balance between the enhancement in mechanical properties and the reduction in energy consumption. Equation (2) is the regression equation that predicts the optimal spot. The optimal parameter settings for attaining the required tensile strength of the HFRE composition sample can be determined via this equation.

Figure 9. Multiple response prediction plots for maximum-tensile-strength O_2plasma-treatedHF-reinforced epoxy composite sample.

The response surface plot and its associated contour plot (Figure 10) show an interaction between the discharge power and treatment time. The elliptical shape of the contour suggests a strong interaction between these two factors, with the maximum tensile strength being achieved at intermediate levels in both parameters.

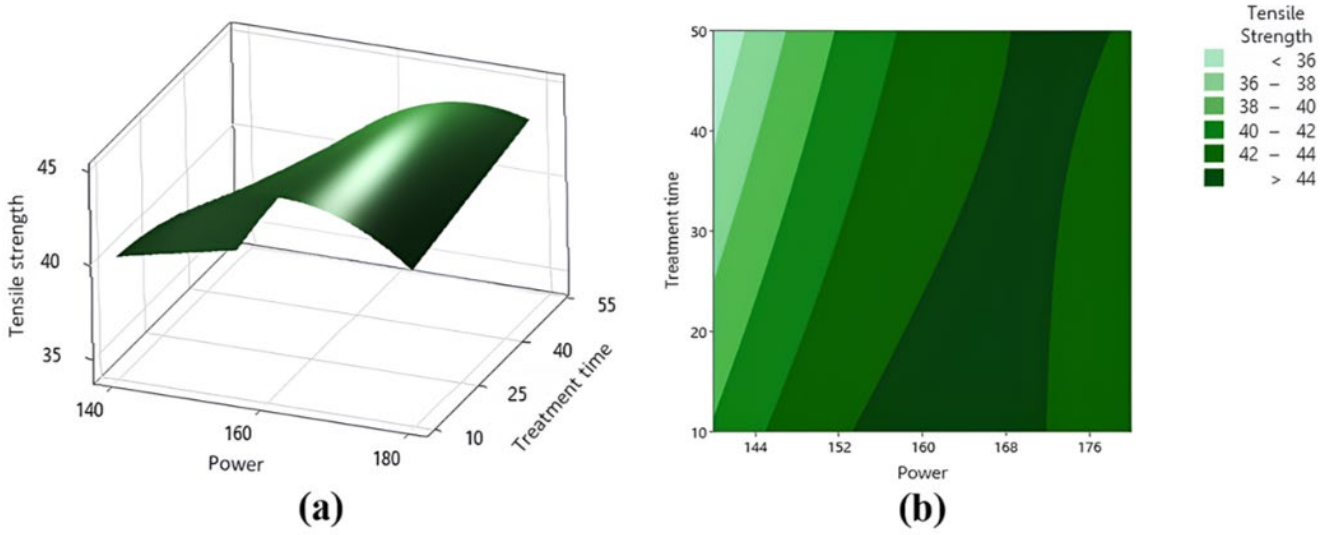

Figure 10. Response curved surface (**a**) and its equal-height line plot (**b**).

Consequently, the RSM optimization allows a maximum of mechanically acceptable properties of the hemp fiber composite to be obtained using the lowest possible energy as a result of plasma treatment. This method could be beneficial towards producing high-performance, environmentally friendly composites for various engineering applications.

4. Discussion

4.1. Mechanism of Crystallinity Enhancement in Cellulose Fibers by Plasma Treatment

The XRD results (Figure 4 and Table 2) show that, after plasma treatment, the crystallinity index increased remarkably for cellulose fibers. There are also other reasons which might be possible sources for this elevated crystallinity; one is the selective etching and removal of amorphous components in the bulk cellulose structure during plasma treatment [6]. Cellulose is a linearly polymerized material at the molecular level that includes crystal line regions separated by disordered amorphous domains [31]. During a plasma treatment, the high energy components such as ions, electrons, and radicals are generated selectively to attack the less stable amorphous regions [32]. The reactive species decompose the amorphous components, and, therefore, a higher relative content of crystalline cellulose was left [25]. The selective etching of the amorphous regions result in a reorganization and alignment of the remaining cellulose chains which drive to form an enhanced degree of order and crystallinity [33]. This reorganization is, in part, due, instead, to the tendency of cellulose molecules to minimize their surface energy and form stable hydrogen bonds [34]

On the basis of experimental observations and literature reports, a model for the crystallinity enhancement in cellulose during plasma treatment can be presented. This model involves several main steps. First is the formation of highly reactive species in plasma, which consists of ions, electrons, and radicals that are generated when plasma interacts with a gas [35]. These species are determined by the plasma gas composition and treatment conditions, both in type and concentration. Secondly, these reactive species can be preferentially targeted to the relatively less stable and disordered amorphous region of cellulose [36]. In this selective etching process, the amorphous components are disintegrated and removed to decrease the amorphous fraction of cellulose. Third, the excited species in plasma transfer energy to cellulose chains so that they can be rearranged locally [16]. This energy transfer will enable the re-orientation of cellulose chains and their alignment to form a better structured fitness. Fourth, the type of reactions is an equivalent depopulation and reorganization process or rearrangement.These changes are related to the disappearance/etching of amorphous regions on cellulose, which have a high surface area are present [37]. That makes the chains line up better and create stronger hydrogen bonds between them, which would yield a more crystalline form. This degree of reorganization depends on the composition of the plasma gas, where reactive gases like oxygen and nitrogen facilitate a more crystalline structure. Finally, the improved hydrogen bonding network and the induced functionalization by reactive gas plasmas (e.g., oxygen-containing groups) stabilize the newly formed crystalline organization [38]. This stabilization discourages cellulose from reverting back to their amorphous state structures. The theory agrees well with the experiments, substantiating a mechanism behind how the crystallinity of cellulose fibers is improved during plasma treatment. This work demonstrates the importance of reactive species, selective etching, energy transfer, and molecular reorganization in accessing a more crystalline cellulose, which presents a process for promoting a greater conversion to cellulose.

4.2. Role of Reactive Oxygen Species (ROS) in Surface Modification of Hemp Fibers During $Ar+O_2$ Plasma Treatment

This study provides evidence of the applicability of plasma treatment as a better choice for the surface modification of hemp fibers. The study found that $Ar+O_2$ plasma treatment produced various ROS, which are important for changing the fiber surface structure of hemp fibers. For example, the ROS that are generated during $Ar+O_2$ plasma treatment have demonstrated a significantly high rate of functionalization on hemp fiber surfaces than other reactive species such as nitrogen species (RNS) or argon-based ones. The ROS,

especially atomic oxygen and ozone, are known to have high oxidation potentials and reactivity towards organic compounds, and have been employed in altering the surface chemistry of hemp fibers [39].

The mechanism of ROS interaction with the fiber component, namely, cellulose, hemicellulose, and lignin, can be described as follows: Firstly, cellulose, the major component of hemp fibers, reacts with different types of ROS, mainly, atomic oxygen and hydroxyl radicals [40]. These species attack the glycosidic bonds of cellulose, resulting in the removal of non-crystalline cellulose and amorphous portions and leading to the predominant appearance of oxygen-containing groups such as −OH and C−O groups on the fiber surface [16,41], where its glycosidic bonds were cleaved by the present fungal strains. This was because the introduction of those polar functional groups increased the surface energy and wettability, which favored their compatibility with polymer matrices [42]. An FT-IR analysis was carried out (Figure 4) The peaks attributed to cellulose were weakened after Ar+O_2 plasma treatment, suggesting that ROS led to the oxidation and modification of the biopolymer. Additionally, hemicellulose, which is an amorphous heteropolysaccharide in hemp fibers with a lower degree of polymerization when compared to cellulose, exhibits a high vulnerability toward oxidative reactions by ROS [43]. This process leads to a higher surface roughness and, effectively, a greater specific area for covalent bonding with polymers [44]. The SEM analysis (Figure 5) showed an increase in surface roughness and the exposure of microfibrils after Ar+O_2 plasma treatment due to the ROS selective ablation of hemicellulose [32]. Lignin, a complex aromatic polymer found in Nutritional Trends that binds cellulose fibrils to one another, is involved as the third layer. ROS formed in the lignin atmospheric plasma treatment (Ar+O_2) can interact with aromatic rings and side chains of lignin to induce oxidative degradation, leading also to the formation of some oxygen functional groups, like phenolic hydroxyl, carboxyl, and carbonyls groups [45]. For example, during the selective isolation of lignin from the fiber surface, it is removed, which exposes cellulose fibrils and increases the surface roughness that will lead to an increase in mechanical interlocking between polymer matrices [46]. In the XRD analysis, as shown in Figure 3 and Table 2, the X-ray diffractograms illustrated an increase in the crystallinity index (C.I.) of the fibers after Ar+O_2 plasma treatment; however, there is still a high contribution from amorphous, lignin, hemicellulose regions, which are removed during the etching process, consequently giving rise to increase portion of the residual crystalline cellulose.

In contrast, RNS formed during nitrogen-containing plasma treatments, such as NH_3 or N_2 plasmas, usually provide amine (NH_2) and imine functional groups (C = N) onto the fiber surface, respectively [47]. Although these groups can increase the compatibility of fibers with certain polymer matrices, inherently hindered and fully stabilized fiber surfaces have much less impact on interfacial adhesion when compared to oxygen-containing surface groups created by ROS [48]. The FT-IR analysis (Figure 4) revealed no significant changes in the Ar and Ar/N_2 plasma-treated fiber spectra, indicative of the involvement of RNS on surface functionalities toward N_2 as compared to ROS.

The processes of argon-based plasma treatments used for surface cleaning and etching prevail in the physical bombardment at the fiber surface by energetic argon ions and electrons [49]. This process can improve the surface roughness and has the effect of removing contaminants, while it does not significantly change the surface chemistry of fibers [50]. Without chemical modification, the argon plasma treatment alone can only enhance interfacial adhesion to a limited extent. The results of this study indicated that the tensile strength and energy absorption plateau stress improved to a lesser extent in the Ar plasma treatment compared to those in the co-treatment with one atmosphere

argon/oxygen, as shown in Figure 7 and Table 3, suggesting the relatively poor performance of argon-based species for surface modification.

4.3. Optimizing DBD Plasma Treatment Parameters and Reactor Design for Efficient Hemp Fiber Surface Modification in Composite Manufacturing

The results of the study, and, in particular, its ANOVA analysis, have provided new insights to highlight the association between plasma parameters with the surface modification efficiency of hemp fibers. The ANOVA results (Table 4) showed that the input power had a significant effect on the tensile strength of epoxy composites reinforced with Ar+O_2 plasma-treated HF, as its *p*-value was recorded around 0.028 (α = 0.05). These results indicate that the tensile strength of composites was raised to a certain degree with an increase in input power, as shown in Figure 10. Overly high powers can cause thermal damage and structural loss of the fiber as well [51]. Surprisingly, the ANOVA test results showed that the tensile strength is not commonly affected by treatment time (*p*-value 0.387). Contrary to the general belief that increased the exposure time results in enhanced surface modifications [52], this observation has been made with some caution. That being said, it is worth noting that although the statistical insignificance of treatment time indicates no effect on surface modification, as it falls within the range of values investigated, there was not as much change in the tensile strength for the time rangingfrom 10–50 min compared to input power.

Therefore, the results of the ANOVA and RSM analysis on this study reinforce that input power was concentratedly dominantly affecting a surface modification of hemp fibers by DBD plasma treatment. The selection of a 162.63 W input power with a treatment time of ten minutes using an Ar+O_2 plasma is recommended under the present conditions, which may enable an improvement in the surface properties of hemp fibers, leading to an enhanced mechanical performance for hemp-fiber-reinforced composites.

Designing an optimal DBD plasma reactor in order to coat natural fibers such as hemp requires considering various features and working parameters that affect the desired surface modification uniformity and efficiency. The configuration of the electrode system, flow dynamics, and scaling up of the reactor become important considerations. The electrode configuration is an important factor affecting plasma characteristics and treatment uniformity when using a DBD plasma reactor. A parallel-plate electrode configuration was employed in this study with the hemp fibers located on an aluminum tray resting over a grounded electrode as shown in Figure 1. The powered electrode was positioned at the top of the fibers, with a 1 mm discharge gap. Such an arrangement permits a uniform electric field distribution and the same plasma exposure along the fiber face [53]. This prevents localized overtreatment and provides for the uniform treatment of the fibers due to the employment of a moving tray system whereby an aluminum tray is reciprocated forward and backward at a speed of 30 cm s^{-1}.

The gas flow dynamics in the DBD plasma reactor are crucial for achieving uniform treatment and avoiding localized overheating or nonuniform modification. The gas stream was oriented parallel to the surface of the fiber at both sides (Figure 1) whereby uniform exposure to the reactive species is maintained. Gas flow rates were optimized for the plasma gas compositions with Ar (8 L min^{-1}) and O_2 (10 sccm). Computational fluid dynamics (CFD) simulations help us to better understand the gas flow patterns that can be achieved, which provide support in optimizing the design of reactors for efficient and homogeneous treatment [54]. In industrial applications of DBD plasma treatment for natural fibers, scalability is a major concern. The reactor design must be modified to accept higher fiber loads and a continuous feed. Utilize a moving tray system to investigate the potential for treating higher volumes of material per pass. Roll-to-roll systems show promise for the

large-area treatment, where fibers are fed continuously between rotating electrodes through a plasma zone, which have also shown promise for large-scale treatment [55].

Several of the process improvements can be applied to increase the activity and controllability, as well as ensure reliability in DBD plasma treatment for hemp fiber surface modification. One large player in ascension is real-time monitoring and control systems of the plasma treatment process, which can greatly enhance the efficiency and consistency. The continuous monitoring of critical parameters such as the voltage, current, and gas flow rates help in making instantaneous corrections to achieve the ideal treatment conditions. The results and discussion show the characterization of the plasma-treated fibers. Our study used the response surface methodology (RSM) to find the best combination for producing composite materials with the maximum tensile strength using hemp-fiber-reinforced epoxy composites, via an approach that consists of the treatment time followed by discharge power for maximizing the tensile strength of hemp-fiber-reinforced epoxy composites (Figure 9 and Table 4). By going a step further and incorporating these conditions into a closed-loop control system, a consistent surface modification across various fiber batches can be achieved with a reduced process variability. Secondly, standardized protocols and quality control measures need to be developed for the successful translation of surface modification at an industrial scale. Therefore, detailed working procedures, especially regarding the fiber preparation, parameters of plasma, and post-treatment, can help decrease the fluctuations in processing. Thus, with the combining of these improvements in a process by taking advantage of optimal conditions explored in this work for designing DBD plasma treatment processes, significant enhancement can be achieved on both efficiency and reproducibility throughout bettering the hemp fiber surface modification. This will enable the industrial use of plasma-treated hemp fiber in high-performance composite applications.

5. Conclusions

DBD plasma treatment, especially with Ar+O_2 plasma, caused considerable changes in the surface properties of HF fibers by etching and oxidizing cellulose molecules into functional groups, increasing crystallinity, and promoting surface roughness. The morphological analysis suggested that the surface modifications greatly enhanced the interfacial adhesion between epoxy resin and hemp fiber, which resulted in increases of 15.2% in tensile strength, while a better energy absorption was observed for HFRE composites than those prepared using untreated fibers. In this system, the role of ROS is significant in the oxidization of cellulose/hemicellulose and lignin components during surface modification. The application of response surface methodology (RSM) for the optimization of plasma treatment parameters revealed that the input power was most significant towards tensile strength in HFRE composites undergoing an atmospheric pressure dielectric barrier discharge and its optimal conditions were 162.63 W input power with a duration time for treatment at 10 min. The electrode configuration, gas flow dynamics, and reactor design scalability can be optimized to enable efficient surface modification in a uniform manner. These process improvements can be utilized to improve the efficiency and consistency of DBD plasma treatment for HF surface modification in industrial-scale composite manufacturing by real-time monitoring, control systems, and standardized protocols. Nonetheless, the results of this experiment will be applied to the researcher's reinforced concrete applications, which will be further studied in the future. Additionally, water absorption, compressive strength, and thermal conductivity are crucial properties for the application of composite materials in construction. These materials may need to survive environments of high humidity or pressure. Therefore, the study of these properties will be studied extensively in the future.

Author Contributions: Conceptualization, C.S., K.J., P.R. and P.W.; methodology, C.S., K.J., P.R. and P.W.; validation, C.S., K.K., T.K. and P.T.; formal analysis, C.S., K.K. and P.R.; investigation, K.K., T.K. and P.T.; resource, C.S., K.J., P.W., P.R. and J.S.; writing—original, C.S., K.K. and K.J.; writing—review and editing, C.S., K.J., P.W., P.R. and J.S.; visualization, C.S., K.K. and P.W.; supervision, C.S., P.R. and P.W.; project administration, C.S. and P.W.; funding acquisition, P.W. All authors have read and agreed to the published version of the manuscript.

Funding: This work was supported by the National Science Research and Innovation Fund (NSRF) via the Program Management Unit for Human Resources & Institutional Development, Research and Innovation [grant number B16F640206]. The present study was partially supported by the Thailand Research Fund (TRF) Research Team Promotion Grant, RTA, Senior Research Scholar (N42A671052).

Institutional Review Board Statement: Not applicable.

Informed Consent Statement: Not applicable.

Data Availability Statement: The original contributions presented in the study are included in the article, further inquiries can be directed to the corresponding authors.

Acknowledgments: We wish to thank the Agriculture and Bio Plasma Technology Center (ABPlas), Science Technology Park (STeP), and Chiang Mai University for the laboratory equipment and resources support under the administration of the Materials Science Research Center, Faculty of Science, Chiang Mai University.

Conflicts of Interest: The authors declare no conflicts of interest.

References

1. Ouajai, S.; Shanks, R.A. Composition, structure and thermal degradation of hemp cellulose after chemical treatments. *Polym. Degrad. Stab.* **2005**, *89*, 327–335. [CrossRef]
2. Ozen, E.; Kiziltas, A.; Kiziltas, E.E.; Gardner, D.J. Natural fiber blend—Nylon 6 composites. *Polym. Compos.* **2013**, *34*, 544–553. [CrossRef]
3. Gholampour, A.; Ozbakkaloglu, T. A review of natural fiber composites: Properties, modification and processing techniques, characterization, applications. *J. Mater. Sci.* **2020**, *55*, 829–892. [CrossRef]
4. Mwaikambo, L.Y.; Ansell, M.P. Mechanical properties of alkali treated plant fibres and their potential as reinforcement materials II. Sisal fibres. *J. Mater. Sci.* **2006**, *41*, 2497–2508. [CrossRef]
5. Brunengo, E.; Conzatti, L.; Utzeri, R.; Vicini, S.; Scatto, M.; Falzacappa, E.V.; Castellano, M.; Stagnaro, P. Chemical modification of hemp fibres by plasma treatment for eco-composites based on biodegradable polyester. *J. Mater. Sci.* **2019**, *54*, 14367–14377. [CrossRef]
6. Pejić, B.M.; Kramar, A.D.; Obradović, B.M.; Kuraica, M.M.; Žekić, A.A.; Kostić, M.M. Effect of plasma treatment on chemical composition, structure and sorption properties of lignocellulosic hemp fibers (*Cannabis sativa* L.). *Carbohydr. Polym.* **2020**, *236*, 116000. [CrossRef]
7. Li, X.; Tabil, L.G.; Panigrahi, S. Chemical Treatments of Natural Fiber for Use in Natural Fiber-Reinforced Composites: A Review. *J. Polym. Environ.* **2007**, *15*, 25–33. [CrossRef]
8. Legras, A.; Kondor, A.; Heitzmann, M.T.; Truss, R.W. Inverse gas chromatography for natural fibre characterisation: Identification of the critical parameters to determine the Brunauer–Emmett–Teller specific surface area. *J. Chromatogr. A* **2015**, *1425*, 273–279. [CrossRef]
9. Conrads, H.; Schmidt, M. Plasma generation and plasma sources. *Plasma Sources Sci. Technol.* **2000**, *9*, 441. [CrossRef]
10. Radetic, M.; Jovancic, P.; Puac, N.; Petrovic, Z.L. Environmental impact of plasma application to textiles. *J. Phys. Conf. Ser.* **2007**, *71*, 012017. [CrossRef]
11. Xi, M.; Li, Y.-L.; Shang, S.-y.; Li, D.-H.; Yin, Y.-X.; Dai, X.-Y. Surface modification of aramid fiber by air DBD plasma at atmospheric pressure with continuous on-line processing. *Surf. Coat. Technol.* **2008**, *202*, 6029–6033. [CrossRef]
12. Gao, M.; Wang, Y.; Zhang, Y.; Li, Y.; Tang, Y.; Huang, Y. Deposition of thin films on glass fiber fabrics by atmospheric pressure plasma jet. *Surf. Coat. Technol.* **2020**, *404*, 126498. [CrossRef]
13. Enciso, B.; Abenojar, J.; Martínez, M.A. Influence of plasma treatment on the adhesion between a polymeric matrix and natural fibres. *Cellulose* **2017**, *24*, 1791–1801. [CrossRef]
14. Kalia, S.; Kaith, B.S.; Kaur, I. Pretreatments of natural fibers and their application as reinforcing material in polymer composites—A review. *Polym. Eng. Sci.* **2009**, *49*, 1253–1272. [CrossRef]

15. Väisänen, T.; Das, O.; Tomppo, L. A review on new bio-based constituents for natural fiber-polymer composites. *J. Clean. Prod.* **2017**, *149*, 582–596. [CrossRef]
16. Peran, J.; Ercegović Ražić, S. Application of atmospheric pressure plasma technology for textile surface modification. *Text. Res. J.* **2019**, *90*, 1174–1197. [CrossRef]
17. Hamad, S.F.; Stehling, N.; Hayes, S.A.; Foreman, J.P.; Rodenburg, C. Exploiting Plasma Exposed, Natural Surface Nanostructures in Ramie Fibers for Polymer Composite Applications. *Materials* **2019**, *12*, 1631. [CrossRef]
18. Alamri, H.; Low, I.M. Mechanical properties and water absorption behaviour of recycled cellulose fibre reinforced epoxy composites. *Polym. Test.* **2012**, *31*, 620–628. [CrossRef]
19. *JIS K 6251-7*; Rubber, Vulcanized or Thermoplastics—Determination of Tensile Stress-Strain Properties. Japanese Standards Association: Tokyo, Japan, 2010.
20. Xu, G.; Shi, X.-M.; Cai, J.-F.; Chen, S.-L.; Li, P.; Yao, C.; Chang, Z.; Zhang, G.-J. Dual effects of atmospheric pressure plasma jet on skin wound healing of mice. *Wound Repair. Regen.* **2015**, *23*, 878–884. [CrossRef]
21. Rezaei, F.; Gorbanev, Y.; Chys, M.; Nikiforov, A.; Van Hulle, S.; Cos, P.; Bogaerts, A.; De Geyter, N. Investigation of plasma-induced chemistry in organic solutions for enhanced electrospun PLA nanofibers. *Plasma Process. Polym.* **2018**, *15*, e1700226. [CrossRef]
22. Mengjin, W.U.; Lixia, J.I.A.; Suling, L.U.; Zhigang, Q.I.N.; Sainan, W.E.I.; Ruosi, Y.A.N. Interfacial performance of high-performance fiber-reinforced composites improved by cold plasma treatment: A review. *Surf. Interfaces* **2021**, *24*, 101077. [CrossRef]
23. Marrot, L.; Lefeuvre, A.; Pontoire, B.; Bourmaud, A.; Baley, C. Analysis of the hemp fiber mechanical properties and their scattering (Fedora 17). *Ind. Crops Prod.* **2013**, *51*, 317–327. [CrossRef]
24. Mosiewicki, M.A.; Marcovich, N.E.; Aranguren, M.I. 4—Characterization of Fiber Surface Treatments in Natural Fiber Composites by Infrared and Raman Spectroscopy. In *Interface Engineering of Natural Fibre Composites for Maximum Performance*; Zafeiropoulos, N.E., Ed.; Woodhead Publishing: Cambridge, UK, 2011; pp. 117–145. [CrossRef]
25. Nurazzi, N.M.; Asyraf, M.R.M.; Khalina, A.; Abdullah, N.; Aisyah, H.A.; Rafiqah, S.A.; Sabaruddin, F.A.; Kamarudin, S.H.; Norrrahim, M.N.F.; Ilyas, R.A.; et al. A Review on Natural Fiber Reinforced Polymer Composite for Bullet Proof and Ballistic Applications. *Polym.* **2021**, *13*, 646. [CrossRef]
26. Mohit, H.; Arul Mozhi Selvan, V. A comprehensive review on surface modification, structure interface and bonding mechanism of plant cellulose fiber reinforced polymer based composites. *Compos. Interfaces* **2018**, *25*, 629–667. [CrossRef]
27. Lee, C.H.; Khalina, A.; Lee, S.H. Importance of Interfacial Adhesion Condition on Characterization of Plant-Fiber-Reinforced Polymer Composites: A Review. *Polymers* **2021**, *13*, 438. [CrossRef]
28. Andrew, J.J.; Srinivasan, S.M.; Arockiarajan, A.; Dhakal, H.N. Parameters influencing the impact response of fiber-reinforced polymer matrix composite materials: A critical review. *Compos. Struct.* **2019**, *224*, 111007. [CrossRef]
29. Hh, M.; Hanoon, A.; Al Zand, A.; Abdulhameed, A.; Al-Sulttani, A. Torsional Strengthening of Reinforced Concrete Beams with Externally-Bonded Fibre Reinforced Polymer: An Energy Absorption Evaluation. *Civ. Eng. J.* **2020**, *6*, 69–85. [CrossRef]
30. Wang, K.; Xie, X.; Wang, J.; Zhao, A.; Peng, Y.; Rao, Y. Effects of infill characteristics and strain rate on the deformation and failure properties of additively manufactured polyamide-based composite structures. *Results Phys.* **2020**, *18*, 103346. [CrossRef]
31. Moon, R.J.; Martini, A.; Nairn, J.A.; Simonsen, J.; Youngblood, J.P.J.C.S.r. Cellulose nanomaterials review: Structure, properties and nanocomposites. *Chem. Soc. Rev.* **2011**, *40*, 3941–3994. [CrossRef]
32. Vesel, A.; Mozetic, M. New developments in surface functionalization of polymers using controlled plasma treatments. *J. Phys. D: Appl. Phys.* **2017**, *50*, 293001. [CrossRef]
33. Zhang, C.; Zhao, M.; Wang, L.; Qu, L.; Men, Y. Surface modification of polyester fabrics by atmospheric-pressure air/He plasma for color strength and adhesion enhancement. *Appl. Surf. Sci.* **2017**, *400*, 304–311. [CrossRef]
34. French, A.D. Idealized powder diffraction patterns for cellulose polymorphs. *Cellulose* **2014**, *21*, 885–896. [CrossRef]
35. Chaiwong, C.; Rachtanapun, P.; Wongchaiya, P.; Auras, R.; Boonyawan, D. Effect of plasma treatment on hydrophobicity and barrier property of polylactic acid. *Surf. Coat. Technol.* **2010**, *204*, 2933–2939. [CrossRef]
36. Kolářová, K.; Vosmanská, V.; Rimpelová, S.; Švorčík, V. Effect of plasma treatment on cellulose fiber. *Cellulose* **2013**, *20*, 953–961. [CrossRef]
37. Wohlfart, E.; Fernández-Blázquez, J.P.; Knoche, E.; Bello, A.; Pérez, E.; Arzt, E.; del Campo, A. Nanofibrillar Patterns by Plasma Etching: The Influence of Polymer Crystallinity and Orientation in Surface Morphology. *Macromolecules* **2010**, *43*, 9908–9917. [CrossRef]
38. Huo, J.; Zhu, B.; Ma, C.; You, L.; Cheung, P.C.-K.; Pedisić, S.; Hileuskaya, K. Effects of chemically reactive species generated in plasma treatment on the physico-chemical properties and biological activities of polysaccharides: An overview. *Carbohydr. Polym.* **2024**, *342*, 122361. [CrossRef]
39. Kusano, Y.; Andersen, T.; Michelsen, P. Atmospheric pressure plasma surface modification of carbon fibres. *J. Phys. Conf. Ser.* **2008**, *100*, 012002. [CrossRef]

40. Huh, Y.-i.; Mensah, B.; Kim, S.; Lee, H.; Nah, C. Effects of Plasma Treatment on Mechanical Properties of Jute Fibers and Their Composites with Polypropylene. *Elastomers Compos.* **2012**, *47*, 310–317. [CrossRef]
41. Kafi, A.A.; Magniez, K.; Fox, B.L. A surface-property relationship of atmospheric plasma treated jute composites. *Compos. Sci. Technol.* **2011**, *71*, 1692–1698. [CrossRef]
42. Inbakumar, S.; Morent, R.; De Geyter, N.; Desmet, T.; Anukaliani, A.; Dubruel, P.; Leys, C. Chemical and physical analysis of cotton fabrics plasma-treated with a low pressure DC glow discharge. *Cellulose* **2010**, *17*, 417–426. [CrossRef]
43. Vesel, A.; Junkar, I.; Cvelbar, U.; Kovac, J.; Mozetic, M. Surface modification of polyester by oxygen- and nitrogen-plasma treatment. *Surf. Interface Anal.* **2008**, *40*, 1444–1453. [CrossRef]
44. Liston, E.M.; Martinu, L.; Wertheimer, M.R. Plasma surface modification of polymers for improved adhesion: A critical review. *J. Adhes. Sci. Technol.* **1993**, *7*, 1091–1127. [CrossRef]
45. Yuan, X.; Jayaraman, K.; Bhattacharyya, D. Mechanical properties of plasma-treated sisal fibre-reinforced polypropylene composites. *J. Adhes. Sci. Technol.* **2004**, *18*, 1027–1045. [CrossRef]
46. Sánchez, M.; Patiño, W.; Cárdenas Pulido, J. Physical-mechanical properties of bamboo fibers-reinforced biocomposites: Influence of surface treatment of fibers. *J. Build. Eng.* **2019**, *28*, 101058. [CrossRef]
47. Gibeop, N.; Lee, D.-W.; Prasad, C.; Toru, F.; Kim, B.; Song, J. Effect of plasma treatment on mechanical properties of jute fiber/poly (lactic acid) biodegradable composites. *Adv. Compos. Mater.* **2013**, *22*, 389–399. [CrossRef]
48. Hua, Z.Q.; Sitaru, R.; Denes, F.; Young, R.A. Mechanisms of oxygen and argon-RF-plasma-induced surface chemistry of cellulose. *Plasmas Polym.* **1997**, *2*, 199–224. [CrossRef]
49. Mahlberg, R.; Niemi, H.E.M.; Denes, F.; Rowell, R.M. Effect of oxygen and hexamethyldisiloxane plasma on morphology, wettability and adhesion properties of polypropylene and lignocellulosics. *Int. J. Adhes. Adhes.* **1998**, *18*, 283–297. [CrossRef]
50. Baltazar-y-Jimenez, A.; Bistritz, M.; Schulz, E.; Bismarck, A. Atmospheric air pressure plasma treatment of lignocellulosic fibres: Impact on mechanical properties and adhesion to cellulose acetate butyrate. *Compos. Sci. Technol.* **2008**, *68*, 215–227. [CrossRef]
51. Yuan, X.; Jayaraman, K.; Bhattacharyya, D. Effects of plasma treatment in enhancing the performance of woodfibre-polypropylene composites. *Compos. Part. A Appl. Sci. Manuf.* **2004**, *35*, 1363–1374. [CrossRef]
52. Kalia, S.; Thakur, K.; Celli, A.; Kiechel, M.A.; Schauer, C.L. Surface modification of plant fibers using environment friendly methods for their application in polymer composites, textile industry and antimicrobial activities: A review. *J. Environ. Chem. Eng.* **2013**, *1*, 97–112. [CrossRef]
53. Kogelschatz, U. Dielectric-Barrier Discharges: Their History, Discharge Physics, and Industrial Applications. *Plasma Chem. Plasma Process.* **2003**, *23*, 1–46. [CrossRef]
54. Jaganathan, S.; Vahedi Tafreshi, H.; Pourdeyhimi, B. A realistic approach for modeling permeability of fibrous media: 3-D imaging coupled with CFD simulation. *Chem. Eng. Sci.* **2008**, *63*, 244–252. [CrossRef]
55. Uehara, T.; Sakata, I. Effect of corona discharge treatment on cellulose prepared from beech wood. *J. Appl. Polym. Sci.* **1990**, *41*, 1695–1706. [CrossRef]